Electronic Supplementary Material (ESI) for Polymer Chemistry.

Crosslinked Siloxane-Silsesquioxane Elastomer with Pyrene Functionalization for Rapid Adsorptions of Benzene, Toluene, and Xylene (BTX) from Water and Sensing of Charged Species

Teeraya Bureerug,[†] Chidchanok Wannasiri,[†] Supphachok Chanmungkalakul,[†] Mongkol Sukwattanasinitt,[§] Vuthichai Ervithayasuporn,[†] and Thanthapatra Bunchuay,[†*]*

[†]Department of Chemistry, Center of Excellence for Innovation in Chemistry (PERCH-CIC), and Center for Inorganic and Materials Chemistry, Faculty of Science, Mahidol University, 272 RAMA VI road, Ratchathewi Bangkok 10400, Thailand.

[§]Department of Chemistry, Faculty of Science, Chulalongkorn University, Bangkok 10330, Thailand

*Corresponding Author: V. Ervithaysuporn (V.E.)

Email: vuthichai.erv@mahidol.edu; maldiniandg@hotmail.com

T. Bunchuay (T.B.)

Email: Thanthapatra.bun@mahidol.edu

Table of contents

Measurements

Fourier-Transform Infrared Spectroscopy (FT-IR) Measurement FT-IR spectra were recorded using the attenuated total reflectance (ATR) technique on a Bruker model Alpha spectrometer.

Solid-state Nuclear Magnetic Resonance Spectroscopy (Solid-state NMR) Solid-state NMR was done with Bruker ASCEND 400 MHz WB NMR/DNP spectrometer for solids.

Spectroscopy (UV-Vis Absorption and Fluorescent Emission Measurement) UV-vis spectroscopy was performed on a UV-vis spectrophotometry (Shimadzu UV-2600), whereas all fluorescence spectra were recorded using a spectrofluorometric technique (Horiba FluoroMax4+, integration time 0.1 s, slit width 2 nm) with Fluoromax software.

Morphological and elemental analysis FESEM imaging and energy-dispersive X-ray elemental analysis were carried out using an FEI Quanta 400 SEM with EDS.

Thermogravimetric analysis (TGA) The TA Instruments SDT 2690 device was used for thermogravimetric analysis (TGA). The thermal stability of the Py-CSSE was analysed under N_2 and O_2 at 20 $^{o}C\ min^{-1}$ from 40 - 800 ^{o}C.

Differential scanning calorimetry (DSC) DSC analyses were conducted by using a DSC 3500 Sirius instrument with heating and cooling rate of 10 $^{o}C\ min^{-1}$ at the temperature range of 50 – 400 ^{o}C

X-Ray Diffractometer (XRD) The X-ray powder diffractograms were obtained on a Bruker AXS X-ray diffractor Model D8 Advance, Germany with Cu radiation, $\lambda = 1.54184\ ^{o}A$. Detector is LYNXEYE_XE_T (1D mode).

Inductively coupled plasma mass spectrometry (ICP-MS) A Perkin Elmer NexION 2000 ICP-MS was used as an element detector. Dara processing was done through the SyngistixTM software.

Compressive test the material was measured by Universal testing machine (INSTRON 5569) with loading force 1 kN. The speed of test as 12 mm/minute. Average size of material: thickness 10.93 mm and diameter 39.64 mm

Synthesis of Mono Pyrene-Functionalized SQ cage (Mono-PySQ)

The synthesis of **Mono-PySQ** was modified from our previously reported methodology. **OVS** (632 mg, 1 mmol), 1-bromopyrene (281 mg, 1 mmol) and triphenylphosphine (26.25 mg, 0.2 mmol) were mixed into a thick- wall and sealed cylindrical vessel with a mixture of THF and Et_3N (8:2 v/v, 10 mL). The solution was deoxygenated by flowing N_2 to the mixture for 10 minutes. Subsequently, $Pd(OAc)_2$ (22.45 mg, 0.1 mmol) was added. The reaction was heated to 80 ^oC and stirred for 48 hours. After the mixture cooled down to room temperature, the solid residues were filtered off and the filtrate was collected, concentrated, and purified via silica-gel column chromatography to afford the pale-yellow powder of **Mono-PySQ** in 20 %yield.

Study of anions and cations sensing

The changes in fluorescent emission were investigated by adding anion or metal into a suspension of 2 mg **Py-CSSE** in 2 ml different media (THF, DMF and DMSO solvent). Fluorescent emission spectra for Py-CSSE in presence of 0.2 mM of different anions TBAX (X = F^-, Cl^-, Br^-, I^-, NO_3^-, CN^-, SCN^-, HSO_4^- and ClO_4^-) and cations as their ClO_4^- salts (Cr^{2+}, Mn^{2+}, Fe^{2+}, Co^{2+}, Cu^{2+}, Zn^{2+}, and Cd^{2+}) ion in 100 µl.

Recyclability of Py-CSSE as an adsorbent for fluoride and cyanide ion

Reusability of **Py-CSSE** was evaluated by adding a solution of TBAF (0.96 mM, 0.4 mL) into a suspension of **Py-CSSE** (10 mg) in THF and standing at room temperature for 5 minutes. After the first cycle of the adsorption process, **Py-CSSE** was removed and the resulting solution was collected and diluted with THF to adjust volume to 0.20 mL. The concentration of fluoride after adsorption was determined by the aforementioned method. The recycled **Py-CSSE** was washed thoroughly with MeOH and stirring in MeOH for 4 hours then dried prior to use in the subsequent cycles. For cyanide adsorption capacity measurements, the experiments were performed similarly to the case of fluoride but the initial concentration of TBACN was adjusted to 0.37 mM.

Study of copper (II) adsorption

Time-dependent adsorption capacity of **Py-CSSE** was determined by using inductively coupled plasma mass spectrometry (ICP-MS) measurements and $CuCl_2$ was used as a source of copper. 10 mg of **Py-CSSE** suspension in 10 mL of THF medium were kept in contact with 0.37 mM of copper by varying reaction times (5, 15, 30, 45, 60, and 75 min). After the adsorption process finished, **Py-CSSE** was separated from each batch via centrifugation. Subsequently, 2 mL of supernatant liquids from each batch were collected carefully, filtered, and dried under reduced pressure, respectively. After that, each batch of **Py-CSSE** was re-dissolved into10 mL of type-I distilled water containing 2% HNO_3 and 5% HCl before getting measured by ICP-MS.

Recyclability of Py-CSSE as an adsorbent for copper ion

To study the recyclability of **Py-CSSE**. For the first cycle, 10 mg of **Py-CSSE** was used and 10 mL of 0.37 mM $CuCl_2$ in THF was added for 10 min. Subsequently, the solution was filtrated and collected carefully in 2 mL. after that the supernatant liquid was dried under reduced pressure before being redissolved in type-I distilled water containing 2% HNO_3/ 5% HCl and measured by ICP-MS. Then, the solid residue of **Py-CSSE** was collected by filtration and dried before adding 0.01 M of EDTA disodium salt solution to remove metal from the polymer. This step was carried out over approximately 3 hours at room temperature. Finally, the polymer was dried under vacuum overnight before studying adsorption for the next cycle. The same procedure was repeated for 2^{nd} to 4^{th} cycles maintaining consistency in protocol and utilizing $CuCl_2$ as a source of Cu throughout the process.

Calculation of the kinetic constant

At the low concentrations, the kinetic constant could be calculated by the following equation:

$$ln[I] = kt + ln[I]_0$$

When I and I_0 were the emission intensity before and after the addition of anions, t is a time (s). Kinetic constant (k) could be calculated from the slope of graph between *ln[I]* against t

Calculation of the ceramic yield

$$\text{Ceramic yield} = \frac{Ceramic\ weight}{original\ polymer\ weight}\ x\ 100$$

Compressive test

In uniaxial compression tests, cylindrical **Py-CSSE** with a 40 mm diameter and 10 mm height was used. The experiment performed with loading force 1 kN. The speed of test as 12 mm/min. The %strain of **Py-CSSE** was calculated by the following equation.

$\%strain = \frac{\Delta L}{L} x100$, where ΔL is the change in length and L is original length.

The stress of **Py-CSSE** was given by the equation as below

$\text{Stress} = \frac{F}{A}$, where F is loading force (N) and A is cross-section area of material (m^2).

Quantitative Analysis

The limit of detection (LOD) and limit of quantitative (LOQ) were calculated from fluorescence titration experiments which according to the equations as below

$$LOD = 3\sigma/S$$

$$LOQ = 10\sigma/S$$

Where, σ is the standard deviation of the response and *S* is the slope of calibration curve.

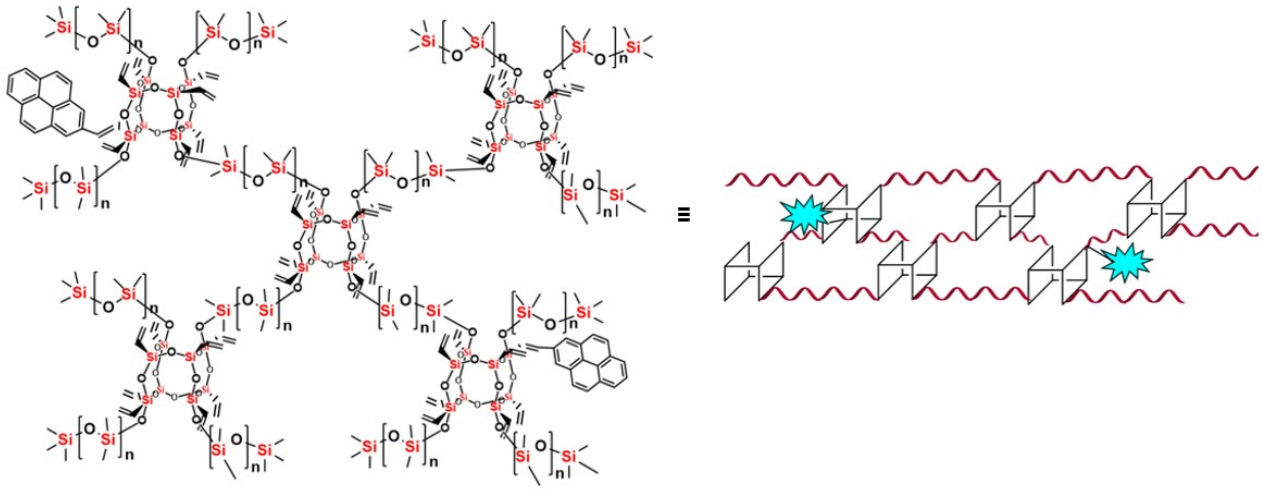

Figure. S1 Structure of **Py-CSSE** material

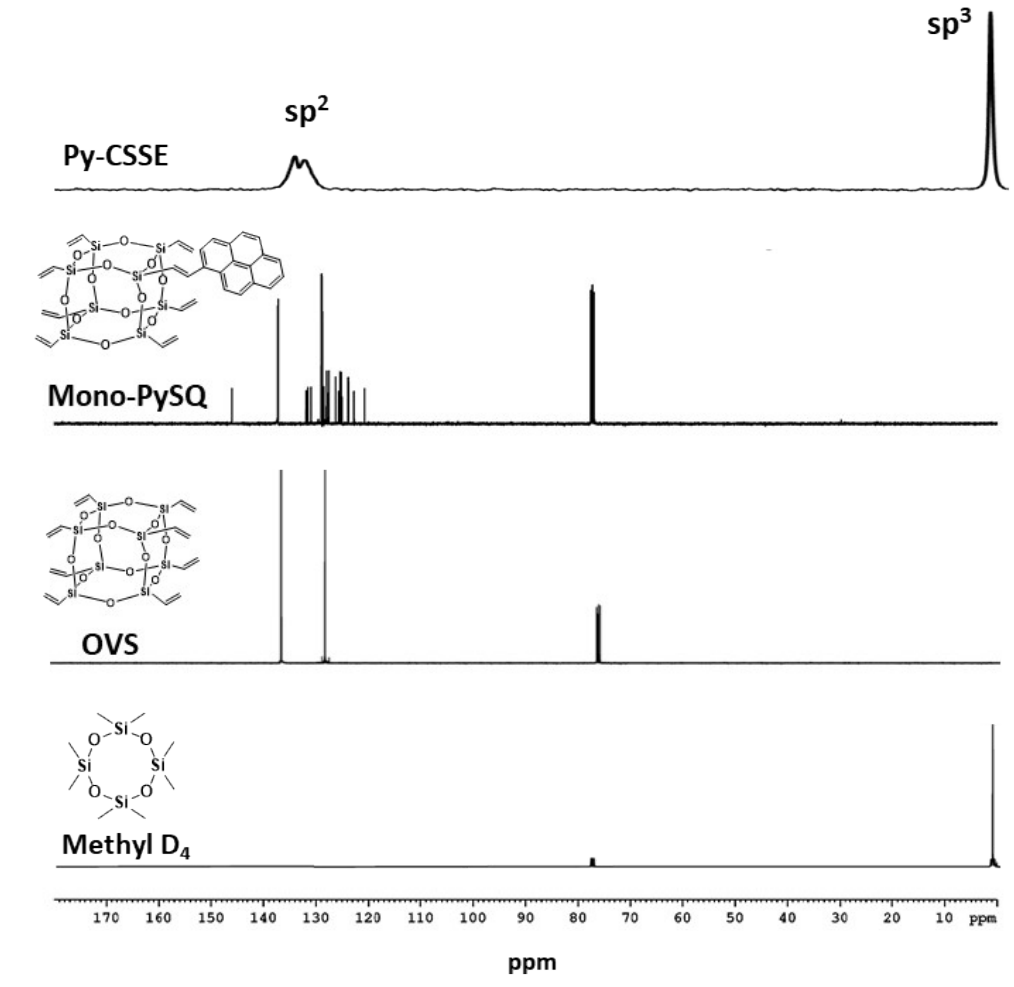

Figure. S2 ^{13}C-NMR spectra of **Mono-PySQ**, **OVS** and **Methyl D_4** in $CDCl_3$ and the solid-state ^{13}C NMR spectrum of **Py-CSSE**

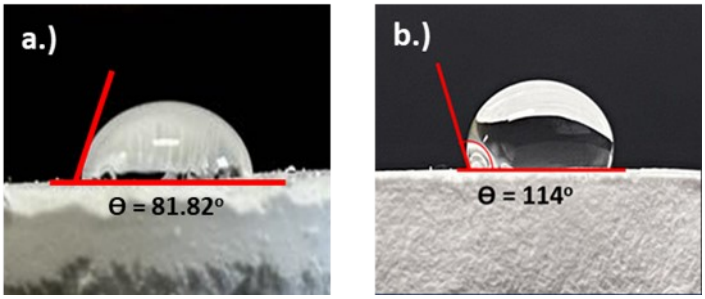

Figure. S3 The contact angle and wettability measurement of **Py-CSSE** (a) without HMDSO modification and (b) with HMDSO modification

Table. S1 FTIR peak assignments

Frequency (cm^{-1})	Vibrational mode
793	Si–O–Si bending
968	*Trans* C=C bending
1072, 1129	Si–O–Si stretching
1260	Si–CH
1406	C–H vinyl bending
1600	Aromatic C=C stretching
2959	C–H stretching
3023	Aromatic C–H stretching
3064	C–H vinyl stretching
3250-3500	OH stretching

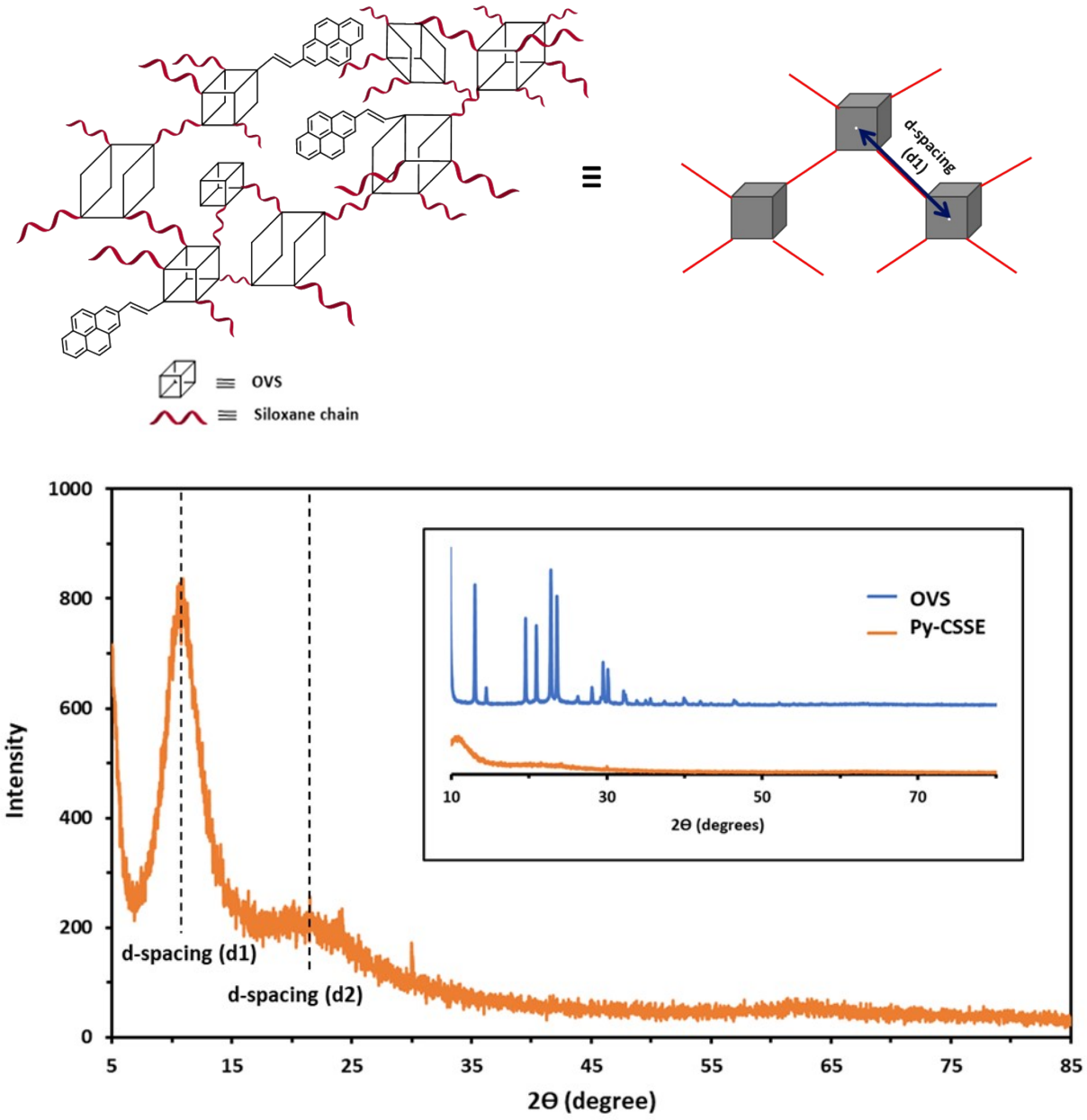

Figure. S4 XRD diffraction curves of **OVS** (Blue) and **Py-CSSE** (Orange) samples

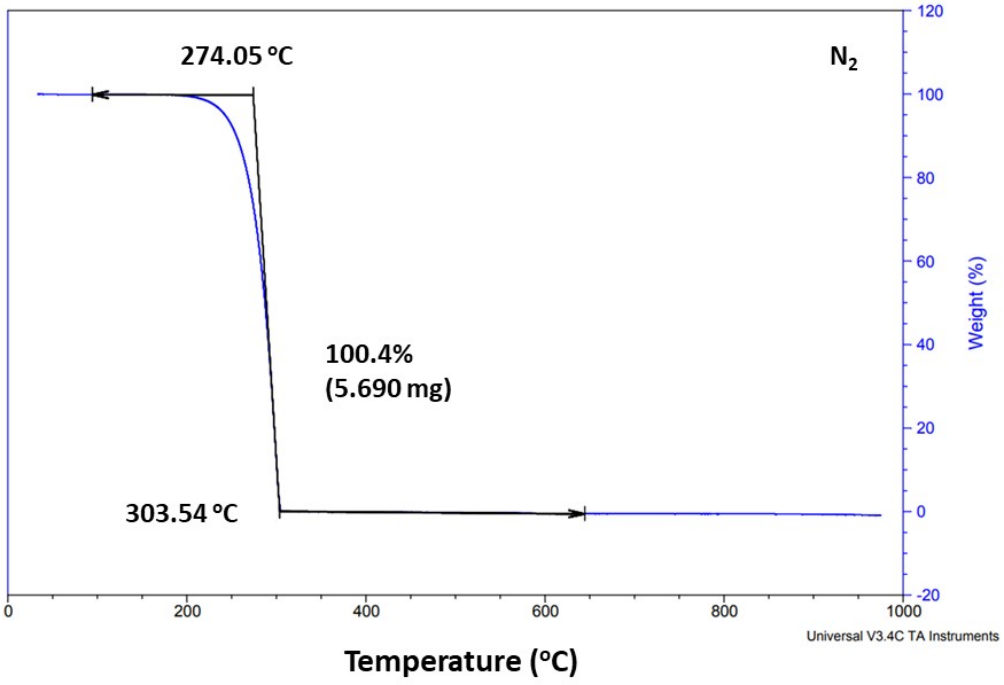

Figure. S5 Thermal gravimetric analysis (TGA) of octavinylsilsesquiloxane (**OVS**) under N_2 atmosphere

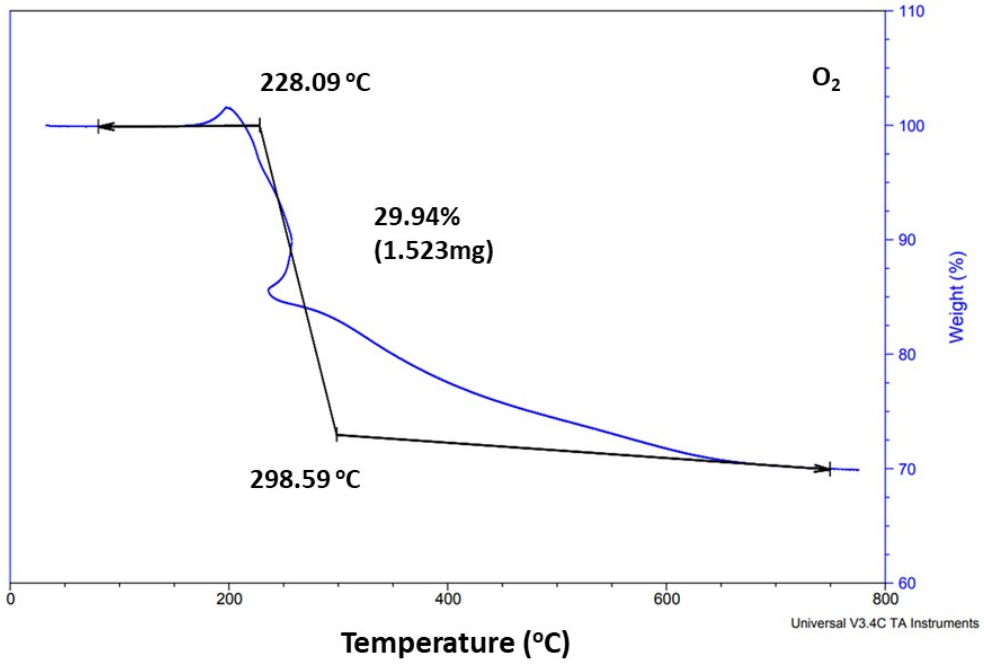

Figure. S6 Thermal gravimetric analysis (TGA) of octavinylsilsesquiloxane (**OVS**) under O_2 atmosphere

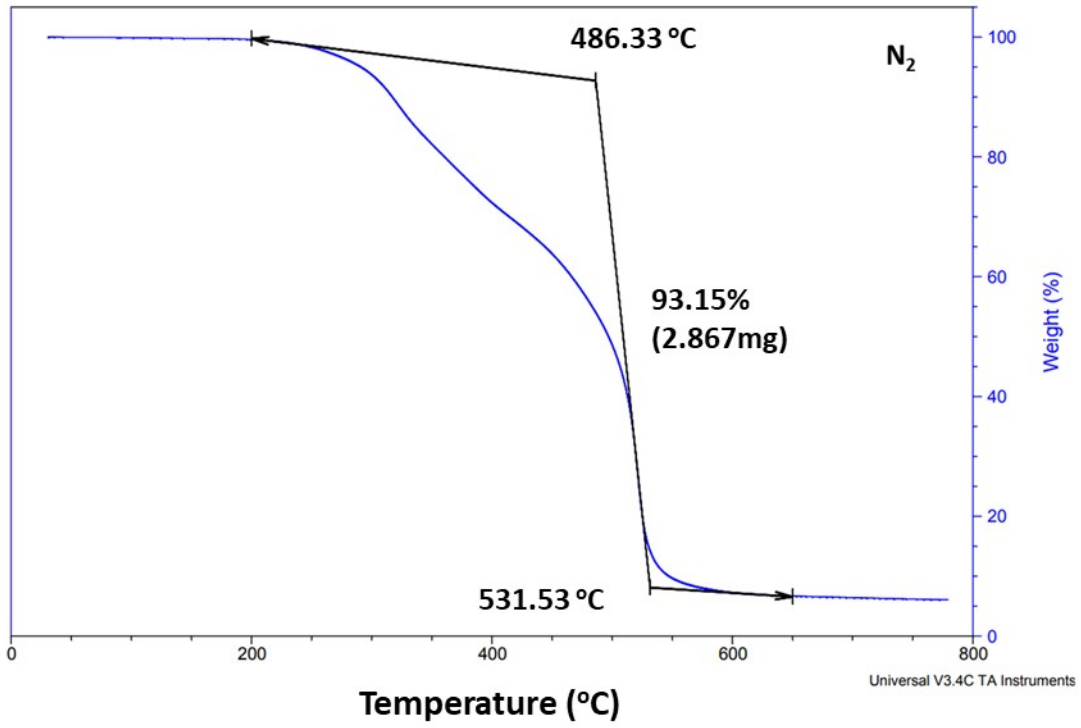

Figure. S7 Thermal gravimetric analysis (TGA) of **Py-CSSE** under N_2 atmosphere

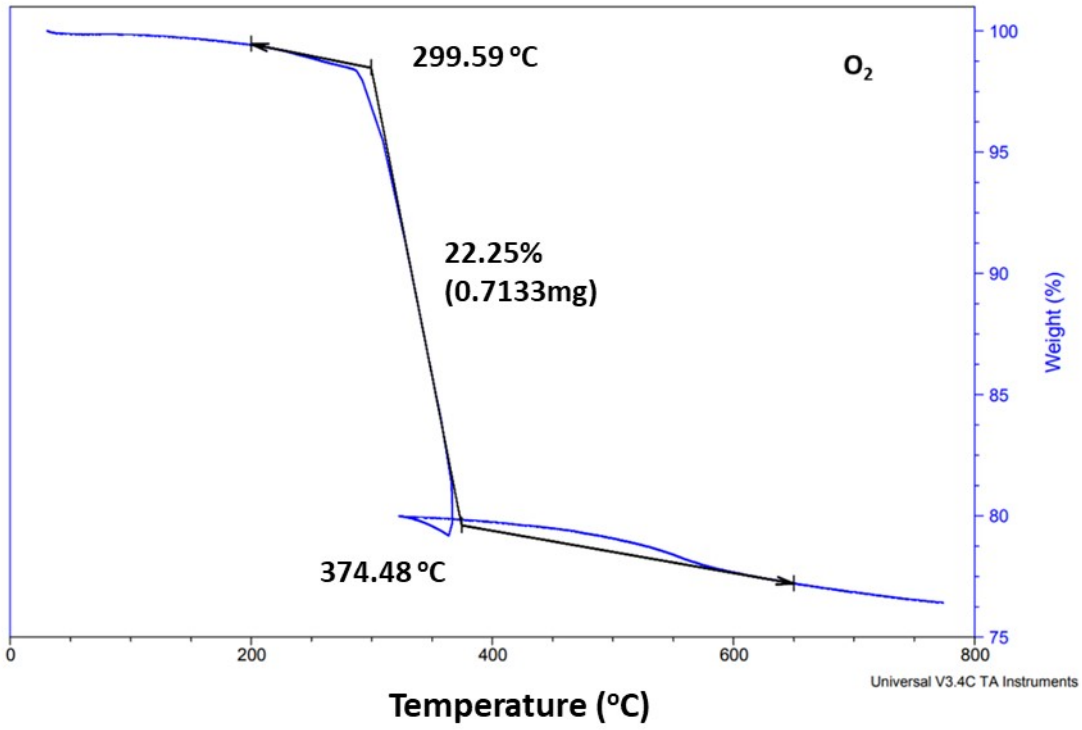

Figure. S8 Thermal gravimetric analysis (TGA) of **Py-CSSE** under O_2 atmosphere

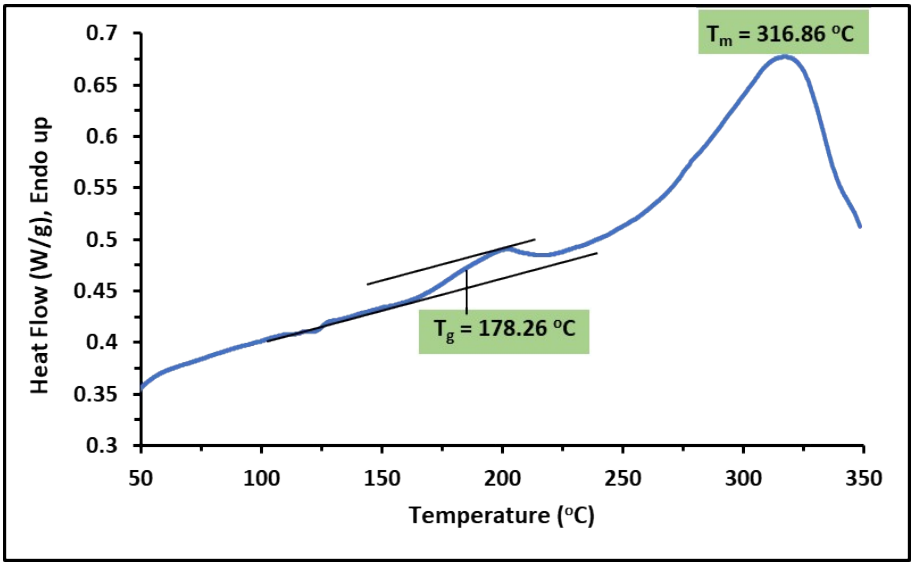

Figure. S9 Differential scanning calorimeter (DSC) heating thermograms of **Py-CSSE**

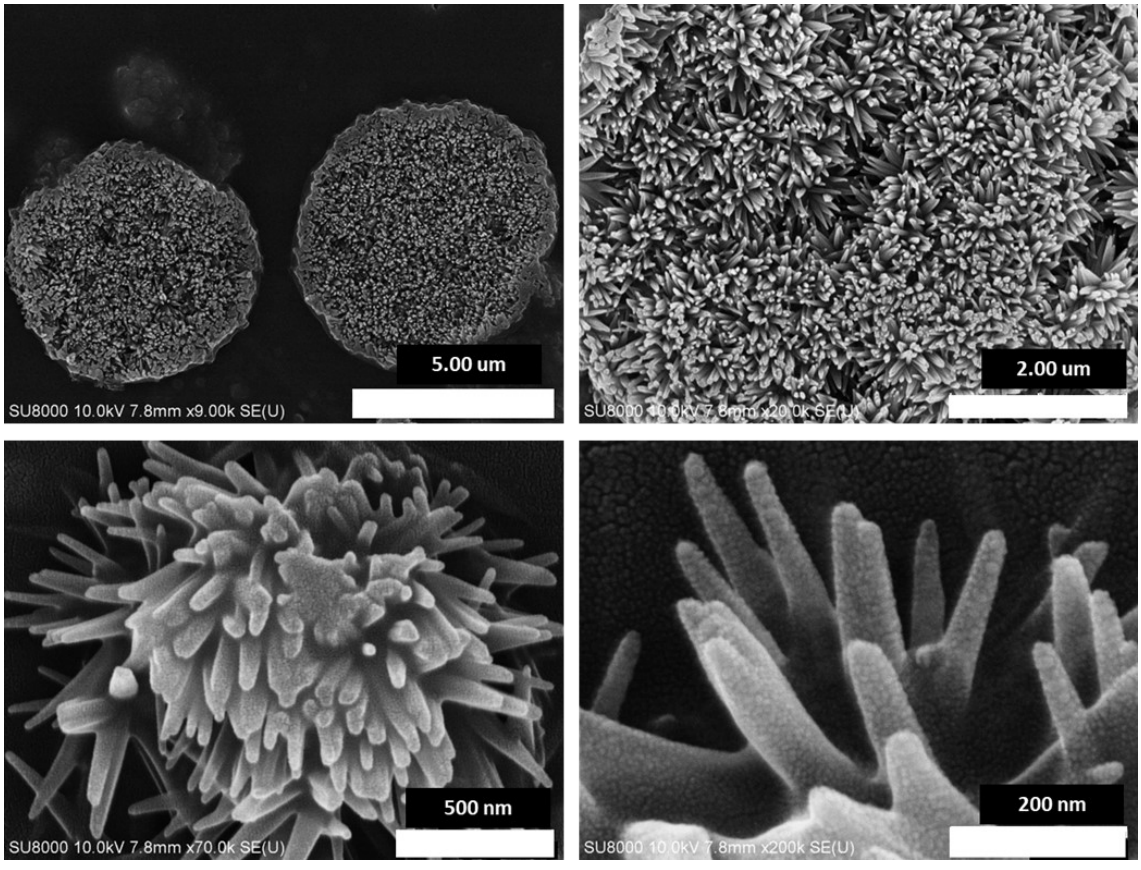

Figure. S10 FESEM images of **Py-CSSE**

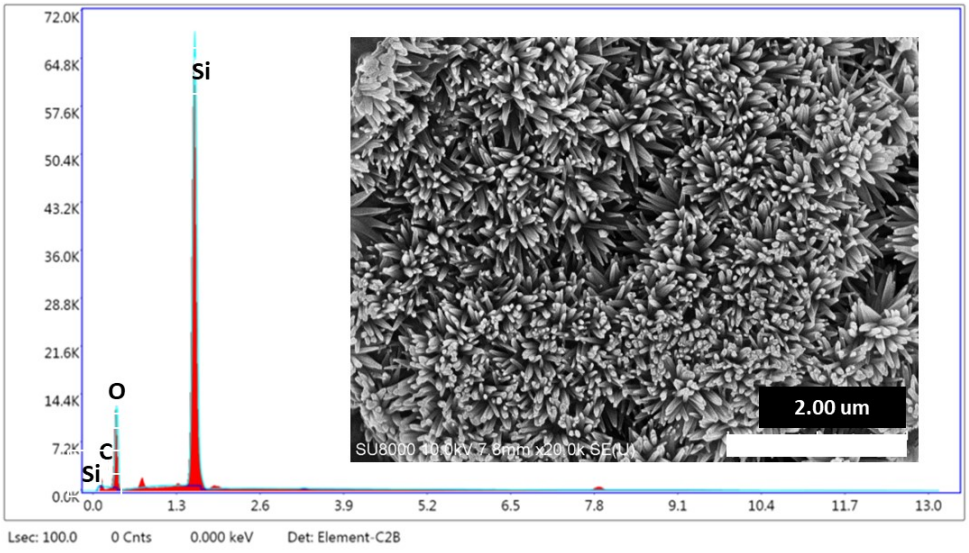

eZAF Smart Quant Results

Element	Weight %	Atomic %	Net Int.
C K	7.83	13.36	36.64
O K	35.15	45.02	735.18
SiK	57.02	41.61	5433.27

Figure. S11 Energy Dispersive X-ray Analysis of a dried sample of **Py-CSSE** suspension in DMF medium.

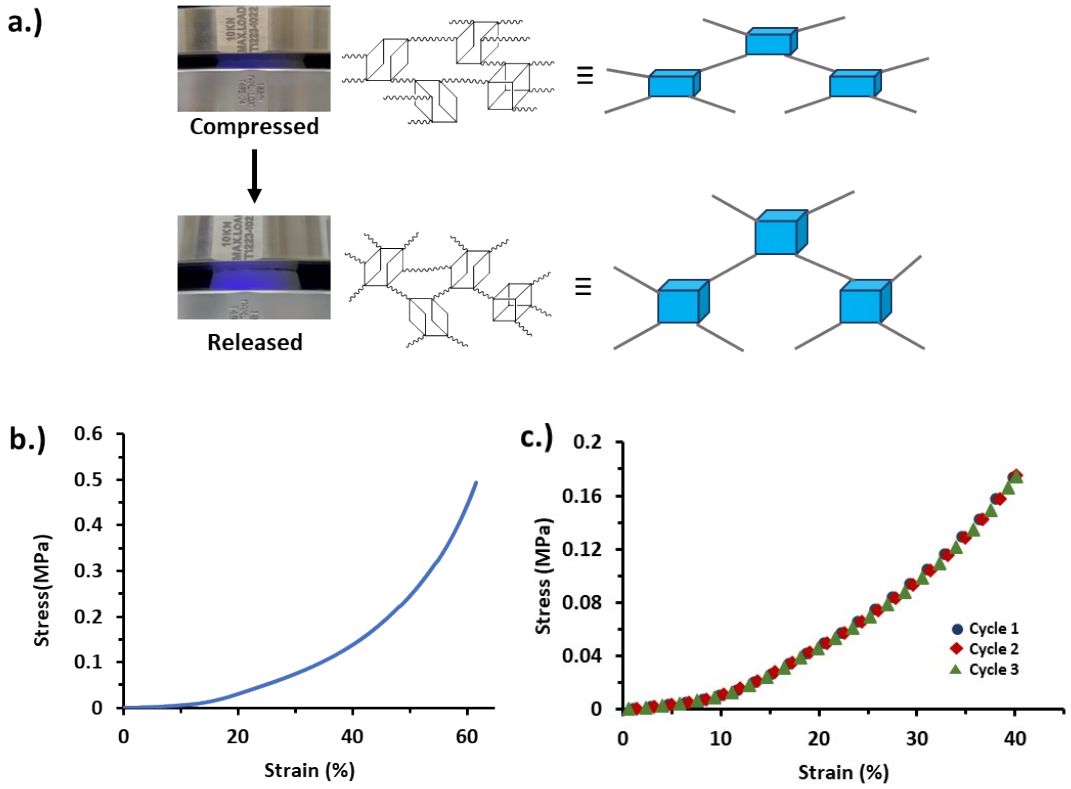

Figure. S12 (a.) Schematic representing the compression-relaxation of **Py-CSSE** at 60% and 0% strain. (b.) The stress-strain curves of **Py-CSSE** structure with cylindrical specimen, obtained from uniaxial compression testing. and (c.) The stress-stain curves for **Py-CSSE** after 3 cycles.

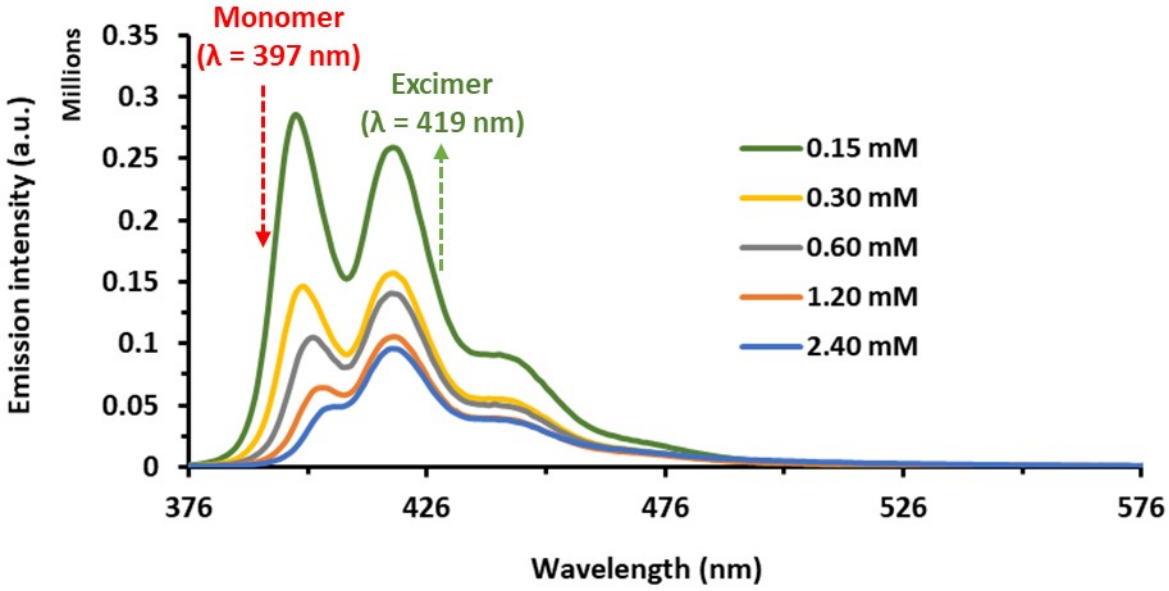

Figure. S13 Concentration-Independent Excimer Formation of **Mono-PySQ** in THF solvent at various concentrations.

Table. S2 Ratio of emission intensity of excimer (λ =419 nm) / monomer (λ =397 nm) in various concentrations.

	Concentration of **Mono-PySQ** in THF				
	0.15 mM	0.30 mM	0.60 mM	1.20 mM	2.40 mM
Ratio of I_{ex}/I_{mo}	0.95	1.27	2.20	4.11	8.64

Table. S3 Adsorption capacity (mol g^{-1}) values of **CSSE** and **Py-CSSE** in different solvent

Solvent	CSSE		Py-CSSE (This work)	
	Average	SD	Average	SD
Hexane	0.0232	0.0003	0.0275	0.0019
THF	0.0438	0.0040	0.0450	0.0018
DCM	0.0424	0.0016	0.0519	0.0034
DMF	0.0173	0.0024	0.0238	0.0033
EtOH	0.0214	0.0012	0.0283	0.0069
MeOH	0.0304	0.0029	0.0334	0.0044
Water	0.0028	0.00009	0.0020	0.0026

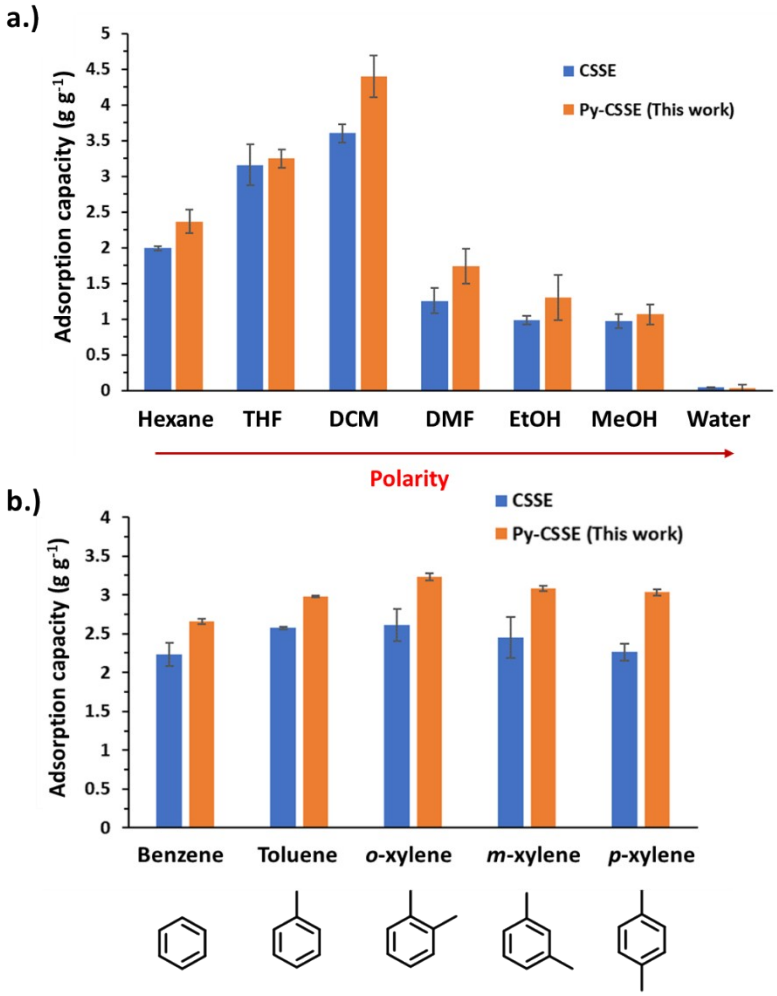

Figure. S14 Adsorption capacities of **Py-CSSE** and **CSSE** towards (a) various solvents reported in g g^{-1} and (b) BTX reported in g g^{-1}.

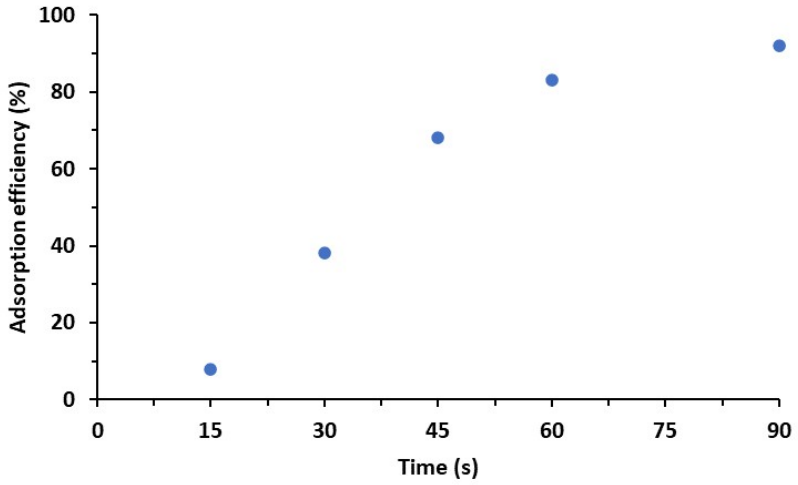

Figure. S15 The time-dependent adsorption capacity of **Py-CSSE** for *o*-xylene adsorption

Table. S4 The BTX adsorption comparison of synthesized materials

Materials	**BTX adsorption**	**Maximum adsorption capacity**	**Ref.**
Organoclays	Benzene Toluene *p*-xylene	0.012 mmol g^{-1} 0.030 mmol g^{-1} 0.140 mmol g^{-1}	1.
Periodic mesoporous organosilica	Benzene Toluene *p*-xylene *o*-xylene	0.6803 mg g^{-1} 0.6601 mg g^{-1} 0.6300 mg g^{-1} 0.6207 mg g^{-1}	2.
SBA-15 from rice husk	Toluene xylene	175.44 mg g^{-1} 142.86 mg g^{-1}	3.
Metal ion-exchanged Y zeolite (NaY zeolite)	*p*-xylene *m*-xylene *o*-xylene	9.76 wt% 11.86 wt% 8.28 wt%	4.
Carbon-based honeycomb monoliths	*o*-xylene	550 µmol g^{-1}	5.
Fe-Al/Bentonite	Benzene Toluene *o*-xylene	175.13 µg g^{-1} 171.84 µg g^{-1} 171.81 µg g^{-1}	6.
Pyrene-functionalized cross-linked siloxane/silsesquioxane elastomer	Benzene Toluene *p*-xylene *m*-xylene *o*-xylene	2.65 g g^{-1} 2.98 g g^{-1} 3.03 g g^{-1} 3.07 g g^{-1} 3.23 g g^{-1}	This work

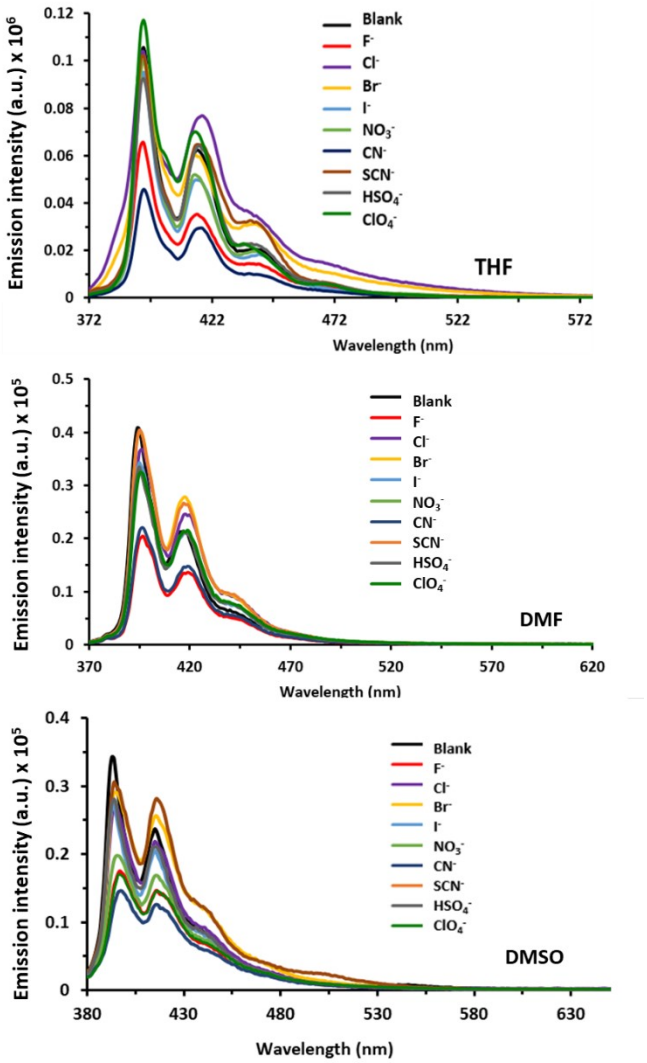

Figure. S16 Fluorescence spectra of **Py-CSSE** (1 mg/mL) in various solvents before and after the addition of 0.2 x 10^{-6} M of anions (50 µl).

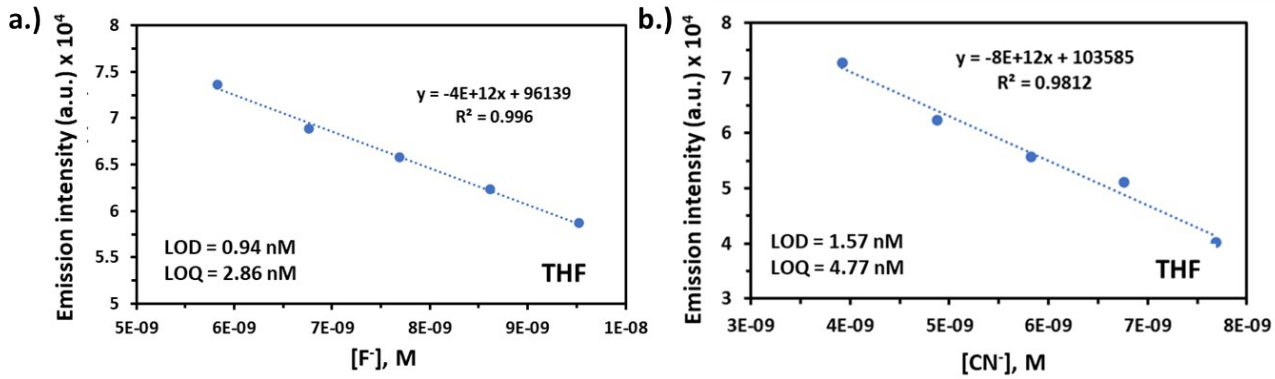

Figure. S17 LOD and LOQ plot from fluorescence titration of **Py-CSSE** (2 mg) with (a.) fluoride ion and (b.) cyanide ion in THF solvents.

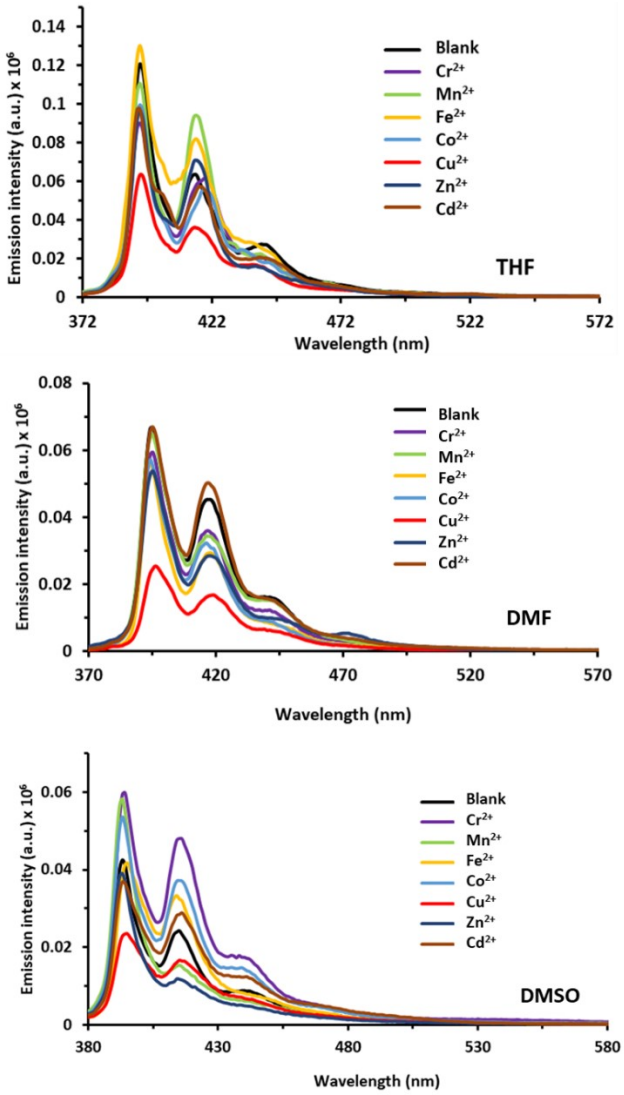

Figure. S18 Fluorescence spectra of **Py-CSSE** (1 mg/mL) in various solvents before and after the addition of 0.2 x 10^{-6} M of cations (50 µl).

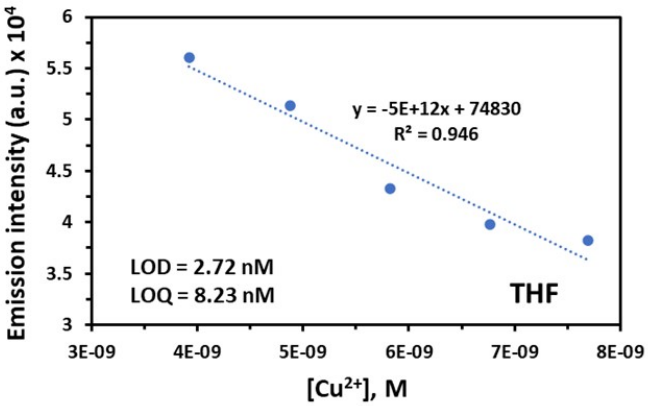

Figure. S19 LOD and LOQ plot from fluorescence titration of **Py-CSSE** (2 mg) with copper ion in THF solvents.

Table. S5 LOD and LOQ of **Py-CSSE** with fluoride, cyanide and copper ions from fluorescence emission titration.

	Fluoride ion (F^-)		**Cyanide ion (CN^-)**		**Copper ion (Cu^{2+})**	
Solvent	**LOD (nM)**	**LOQ (nM)**	**LOD (nM)**	**LOQ (nM)**	**LOD (nM)**	**LOQ (nM)**
THF	0.94	2.86	1.57	4.77	2.72	8.23
DMF	2.46	7.46	1.58	4.80	1.65	4.99
DMSO	4.14	12.54	2.55	7.74	2.04	6.18

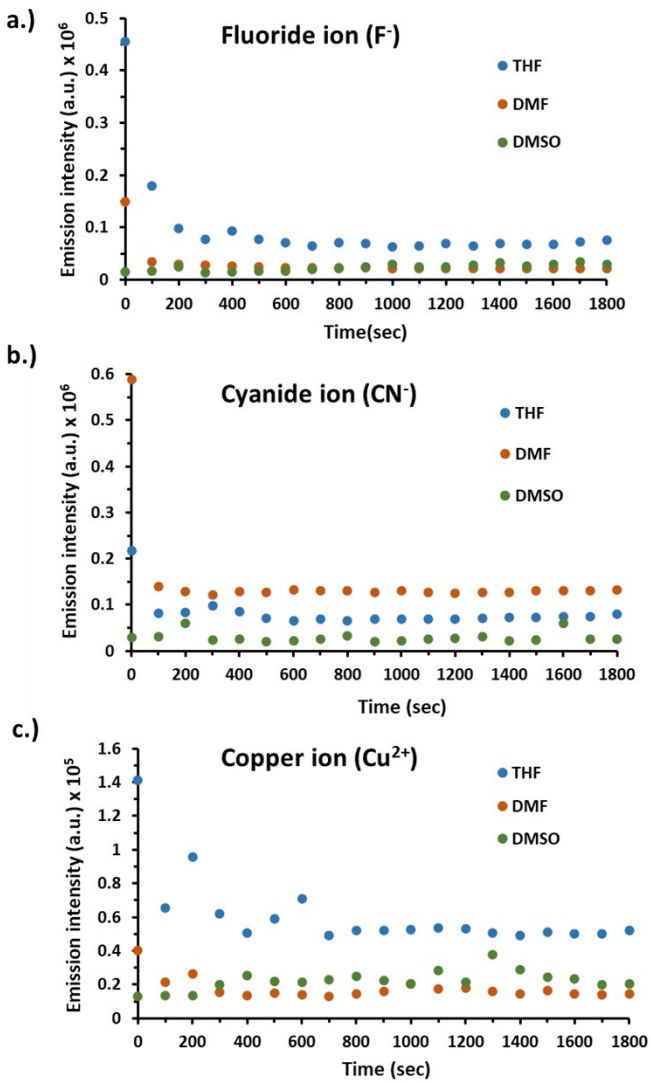

Figure. S20 The kinetics of **Py-CSSE** (1 mg mL^{-1}) upon excessive addition of a.) TBAF b.) TBACN and c.) $Cu(ClO_4)_2$ 0.2 x 10^{-6} M 50 µl in various solvents

Table. S6 Kinetic constant of the reaction between **Py-CSSE** with anions (F^- and CN^-) and metal (Cu^{2+}) in different media

Kinetic constant (*k*) x 10^{-3} sec^{-1}			
Solvent	**F^-**	**CN^-**	**Cu^{2+}**
THF	2.1	8.8	5.1
DMF	2.5	1.5	6.5
DMSO	1.5	3.9	4.2

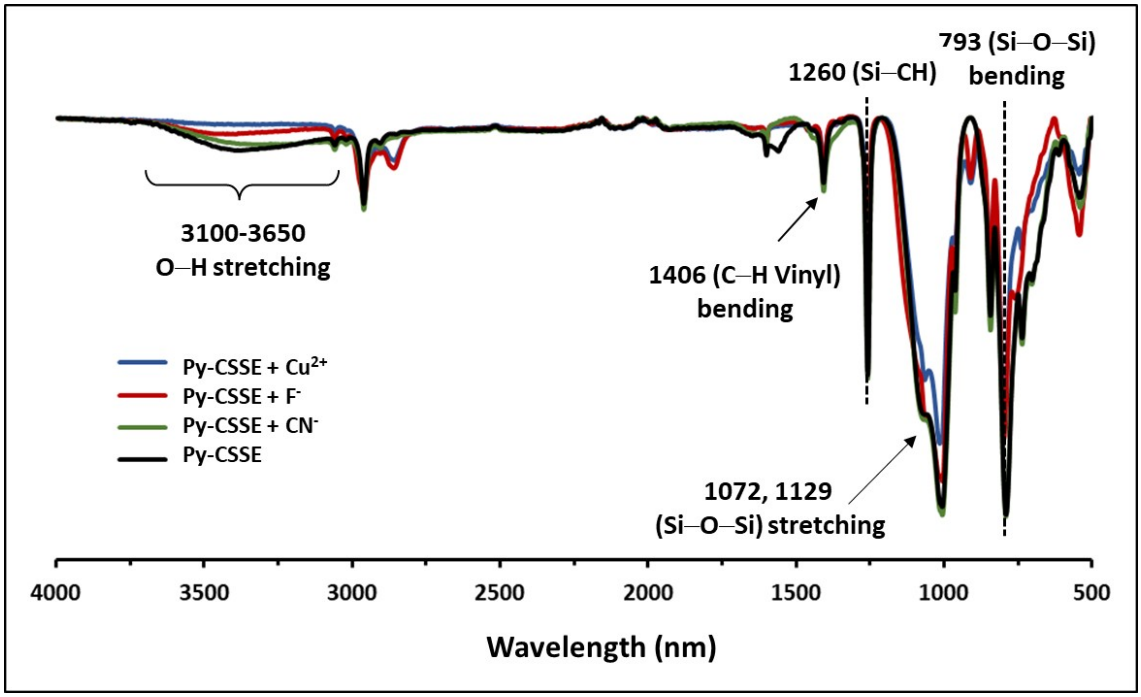

Figure. S21 FTIR spectra of **Py-CSSE** before and after ion addition

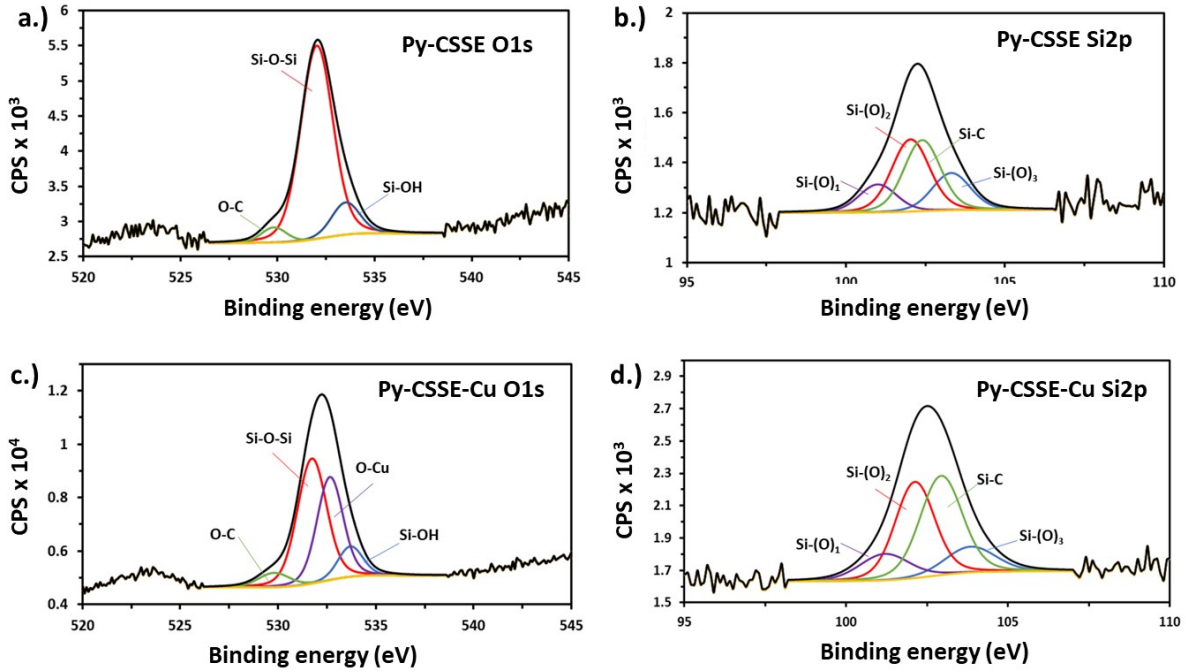

Figure. S22 XPS spectra of **Py-CSSE** a.) O1s b.) Si 2p and **Py-CSSE+Cu^{2+}** c.) O1s d.) Si 2p

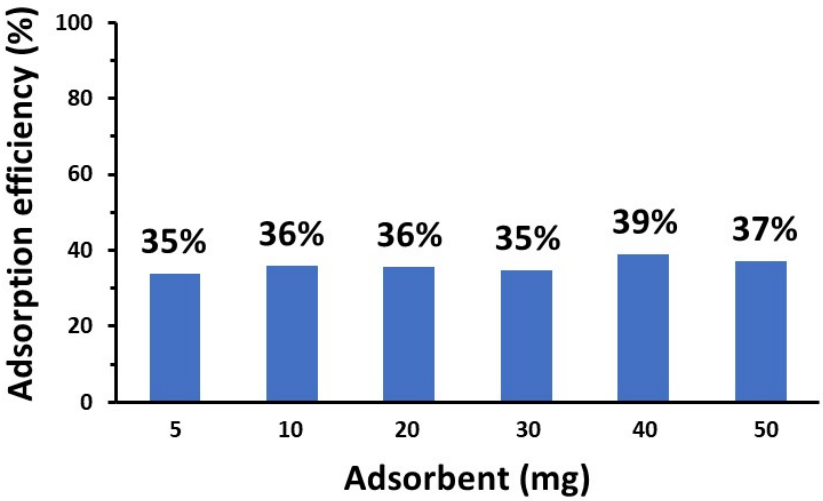

Figure. S23 The Cu^{2+} adsorption efficiency of **Py-CSSE** by varying amounts of adsorbent

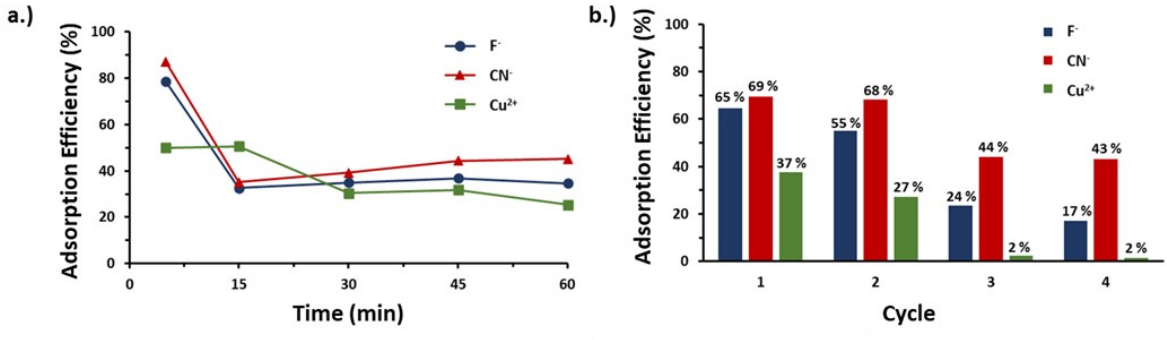

Figure. S24 (a) The time-dependent adsorption efficiency. (b) The reusability of **Py-CSSE** (Adsorption dose, 10 mg; Concentration: F^- (0.96 mM) CN^- (0.37 mM) and Cu^{2+} (0.37 mM) ions.) in THF solvent

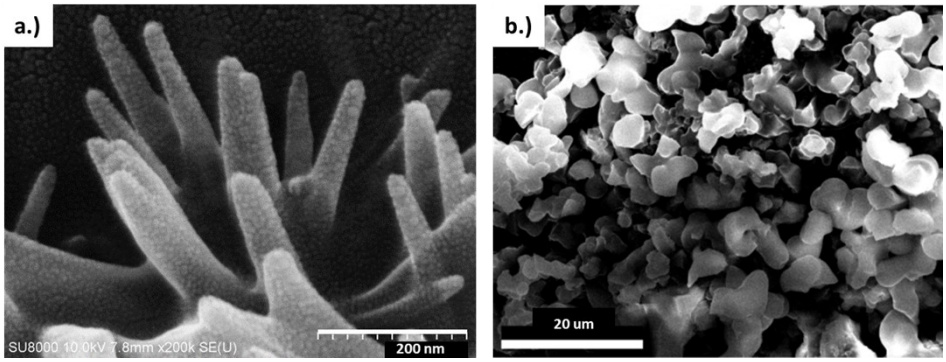

Figure. S25 FESEM image of a dried sample of **Py-CSSE** (a) before and (b) after Cu^{2+} addition

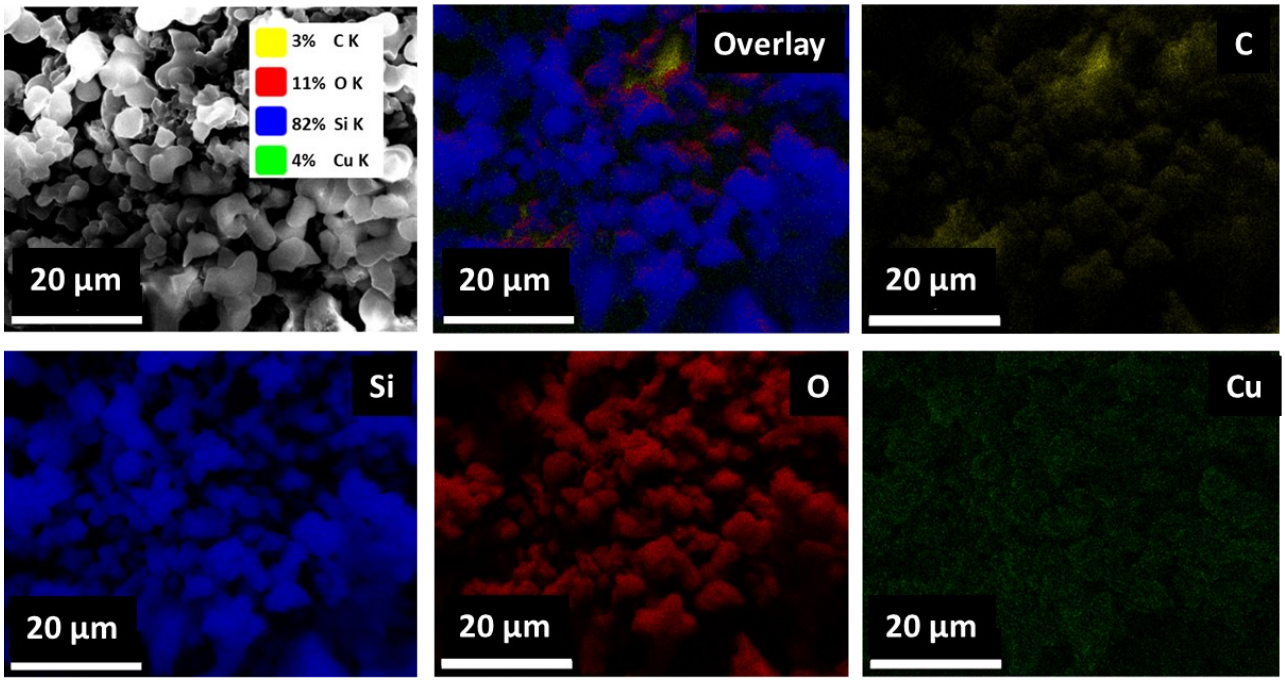

Figure. S26 Elemental mapping of a dried sample of **Py-CSSE** that had adsorbed Cu^{2+} ions

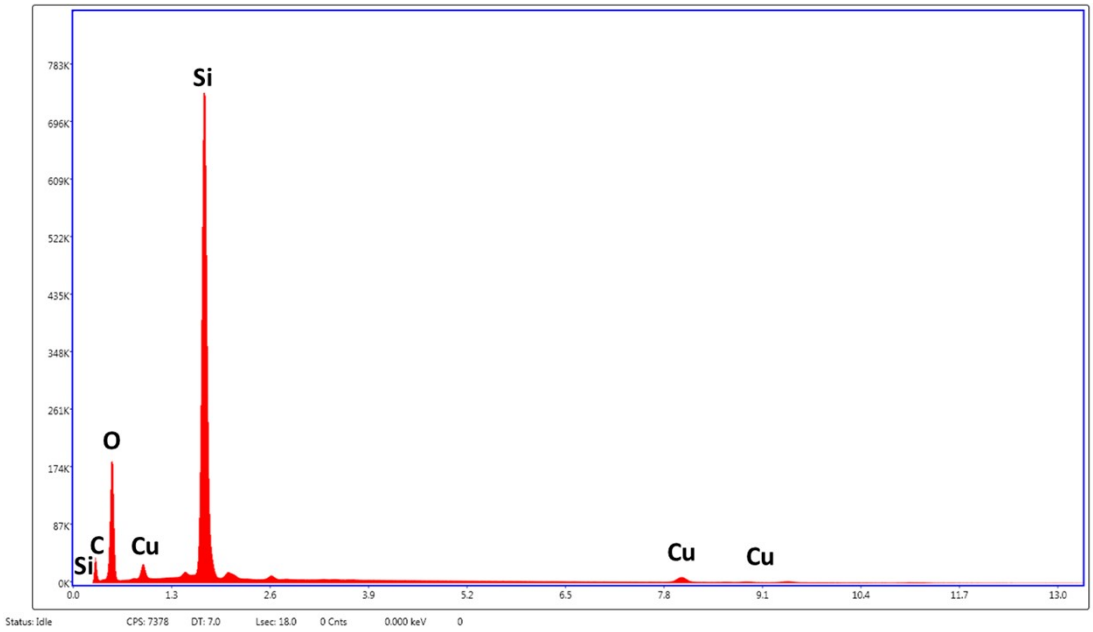

eZAF Smart Quant Results

Element	Weight %	Atomic %	Net Int.	Error %	Kratio	Z	A	F
C K	12.64	20.76	78.71	10.28	0.01603648	1.0905	0.1164	1.0000
O K	36.45	44.95	880.46	8.61	0.09148939	1.0447	0.2402	1.0000
SiK	47.18	33.14	4936.32	2.90	0.3650796	0.9513	0.8129	1.0007
CuK	3.73	1.16	82.78	3.18	0.03205944	0.7672	1.0095	1.1095

Figure. S27 Energy Dispersive X-ray Analysis of a dried sample of **Py-CSSE** that had adsorbed Cu^{2+} ions

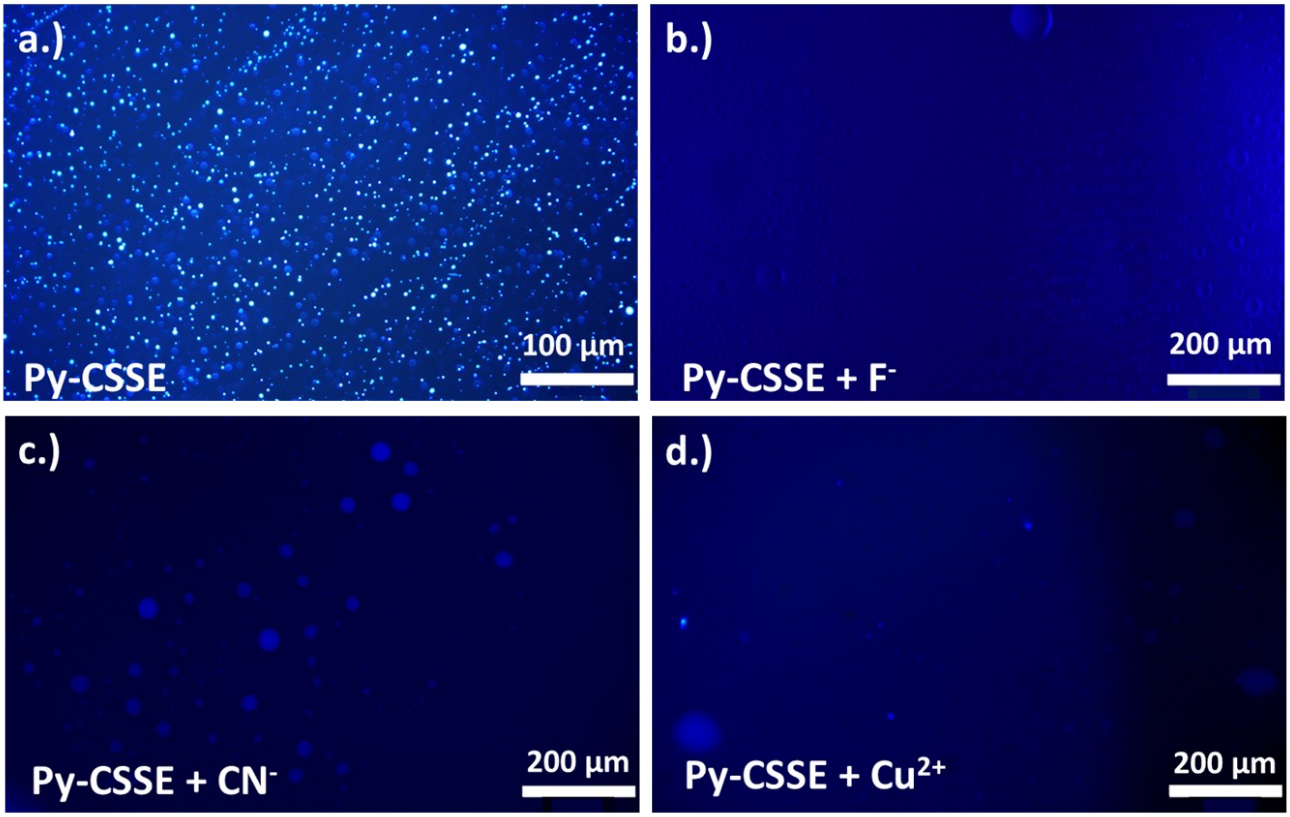

Figure. S28 Epifluorescence microscopy of a.) **Py-CSSE** b.) **Py-CSSE+F$^-$** C.) **Py-CSSE+CN$^-$** and d.) **Py-CSSE+Cu^{2+}** in DMF

Supplementary Movies

Video S1. This video shows the synthesis of **Py-CSSE**.

References

1. L. F. Lima, J. R. de Andrade, M. G. C. da Silva and M. G. A. Vieira, Industrial & Engineering Chemistry Research, 2017, 56, 6326-6336.

2. C. P. Moura, C. B. Vidal, A. L. Barros, L. S. Costa, L. C. G. Vasconcellos, F. S. Dias and R. F. Nascimento, Journal of Colloid and Interface Science, 2011, 363, 626-634.

3. Y. Prestianggi, N. Maylisa, R. D. Subagyono and S. Sitorus, 2019.

4. P. Lahot, M. Rani and S. Maken, Brazilian Journal of Chemical Engineering, 2014, 31, 497-502.

5. J. M. Gatica, J. M. Rodríguez-Izquierdo, D. Sánchez, T. Chafik, S. Harti, H. Zaitan and H. Vidal, Comptes Rendus Chimie, 2006, 9, 1215-1220.

6. Z. Mèçabih, Journal of Encapsulation and Adsorption Sciences, 2017, 7, 40.